Background errors in HIRLAM variational data assimilation

Magnus Lindskog[1], Ole Vignes[2], Nils Gustafsson[1], Tomas Landelius[1], Sigurdur Thorsteinsson[3] and other HIRLAM researchers

[1]*Swedish Meteorological and Hydrological Institute (SMHI)*
[2]*Meteorologisk Institutt*
[3]*Icelandic Meteorological Office*

1. Introduction

The data assimilation system of HIRLAM is based on a variational approach (Gustafsson *et al*., 2001; Lindskog *et al*., 2001). The HIRLAM 3-dimensional variational data assimilation (3D-Var) system became operational in 2000 and HIRLAM 4-dimensional variational data assimilation (4D-Var) is planned to become operational in 2007. An incremental formulation (Courtier *et al*., 1994) is used and the assimilation consists in finding the model state increment vector that minimizes the following cost function problem:

$$J = J_b + J_o = \frac{1}{2}\delta x^T \mathbf{B}^{-1}\delta x + \frac{1}{2}(\mathbf{H}x^b + \mathbf{H}_{tl}\,\delta x - y)^T \mathbf{R}^{-1}(Hx^b + H_{tl}\delta x - y) \tag{1}$$

where **B** is the matrix containing the covariances of the background field errors and **R** is a matrix containing the covariances of the errors in the observations. Furthermore, T denotes the transpose, or adjoint. The non-linear observation operator **H** and the tangent-linear observation operator $\mathbf{H}_{tl}$ transform the background state and assimilation increments, respectively, into the observed quantities. The HIRLAM model state increment vector, δx, includes the following model state increment variables to be determined by the variational assimilation:

$$\delta x = x - x^b = \left(\delta u \quad \delta v \quad \delta T \quad \delta q \quad \delta \ln p_s\right)^T \tag{2}$$

where δu is the increment vector of the wind component in the x-direction, δv the wind component increment in the y-direction, δT the temperature increment, δq the specific humidity increment and $\delta \ln p_s$ the increment of the logarithm of the surface pressure.

A pre-conditioning is applied for the HIRLAM 3D-Var through a series of transforms, U that is applied to

$$\chi = U\delta x \tag{3}$$

the assimilation increments:

These transformations constitute the so called background error constraint and it results in an assimilation control variable vector, χ for which the background error covariance matrix can be assumed to be a unit matrix. The transformations include 2-dimensional (horizontal) Fourier transforms to control variables in spectral space. These transforms means that spectral components representing different horizontal wave numbers are statistically independent under the assumption that the spatial correlations are horizontally homogenous.

In addition to J_b and J_o HIRLAM 4D-Var also include a J_c-term, preventing high frequency variations due to gravity waves.

In the next section the HIRLAM static background error statistics is described in more detail, followed by a description of flow dependent aspects in Sections 3 and 4. Finally a summary is presented in Section 5.

2. Static structure functions

Usually the structure functions of HIRLAM are estimated from differences of forecasts at different ranges, but valid at the same time. This is the so-called NMC-method (Parrish and Derber, 1992). An interesting alternative that also has been tried is to derive the forecast error covariances from ensemble assimilation experiments (Houtekamer *et al*., 1996) by perturbing observations and lateral boundaries. Furthermore, regardless of whether the 'NMC-method' or ensemble assimilation is used the balances between the different model variables within the background error constraint may be formulated in terms of an analytical balance (Gustafsson *et al*., 2001) or statistical balance formulation (Berre, 2000). Advantages of the statistical balance are that there are scale and latitude dependent geostrophy, boundary layer friction, and that moisture effects are represented.

For the present reference HIRLAM system, the background error standard deviations within the minimization of the cost function are represented by one vertical profile of each type of variable contained within the background error statistics. These vertical profiles are obtained by horizontal averaging of the values obtained with the NMC method or ensemble assimilation. To become more in accordance with observed innovation statistics the vertical profiles are scaled with a constant scaling factor and also a slight seasonal variation is introduced. There is however no temporal nor horizontal variation of background error standard deviations in the reference HIRLAM assimilation system.

Three different sets of structure functions have been generated and compared:

- The NMC-method was applied on +24 h and +48 h operational HIRLAM forecasts for a data set covering the period 1 December 1997 through 28 February 1998, using an analytical balance. The operational SMHI HIRLAM was applied with a resolution of 0.4^o x 0.4^o in the horizontal and with 31 vertical levels.

- The NMC method was applied on 4 months (August-November 2004) of SMHI operational forecast differences (36 h-12 h). The operational forecast model was run with 22 km horizontal resolution and 40 vertical levels. A statistical balance formulation was used

- The forecast differences were taken from 2 weeks of 6 h forecasts (18 -31 October 2000). These were from an ensemble assimilation experiment. It was carried out at 22 km horizontal resolution and with 40 vertical levels. There were 10 members plus control in the ensemble assimilation experiment (using perturbed observations and perturbed lateral boundaries from a similar experiment at ECMWF). When calculating structure function statistics the members were combined (co-1,1-2,2-3,.....,9-10,10-co) to give 154 cases. Again a statistical balance formulation was used.

The structure functions are illustrated in Figure 1, which shows the horizontal impact of one single surface pressure observation 5 hPa less than the corresponding background equivalent on the surface pressure and low level wind fields. With the new structure functions, using a statistical balance, the frictional inflow associated with a level cyclonic circulation is represented. The horizontal scales of the increments are significantly smaller in the case of ensemble based structure functions.

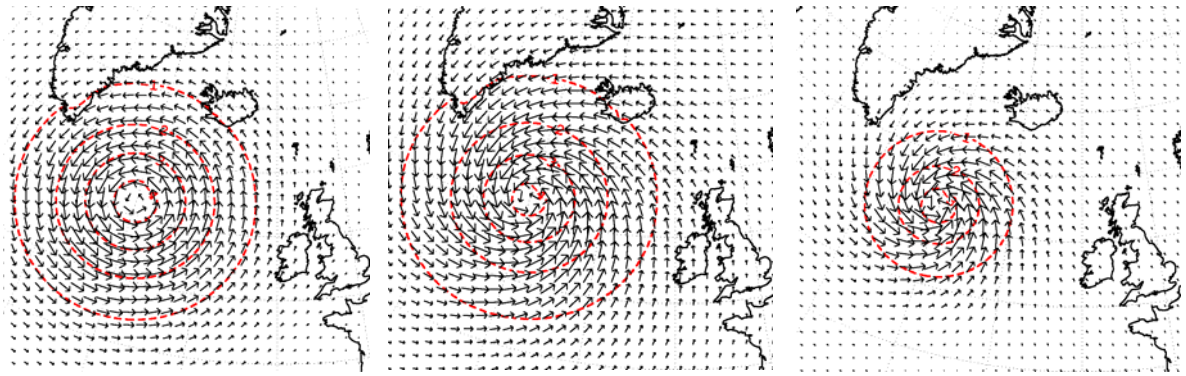

Figure 1: Impact of one single surface pressure observation 5 hPa less than the corresponding background equivalent. Red isolines represent surface pressure increments and black arrows winds at the lowest model level. Left is for reference structure functions (using analytical balance), middle for new NMC-based (using statistical balance) and right for ensemble based (using statistical balance).

Three one month parallel assimilation and forecast experiments have been carried out over a domain covering the Northern mid-latitudes using 3D-Var. The three parallel runs were identical, except for that different structure functions were used (as described above). The structure functions based on statistical balance results in better forecast quality than the structure functions based on analytical balance. There were no significant differences in forecast quality between the run based on new NMC-based and new ensemble based structure functions, using statistical balance. Based on the results like the one from this parallel experiment the old structure functions of the HIRLAM reference system, (NMC based calculated from differences of 24 h and 48 h forecasts using an analytical balance), was replaced by newer ones (also NMC based but derived from differences of 12 h and 36 h forecasts using a statistical balance).

3. Flow dependent background error standard deviations

A first step towards representation of flow dependency of background errors is the introduction of a horizontally varying climatological background error standard deviation field. The climatological index field is introduced with the purpose to represent horizontal variations of the background error standard deviation due to time invariant station density and due to time average baroclinicity. It is calculated using innovations of surface pressure observations from SYNOP, SHIP and DRIBU reports. The innovations were retrieved from operational 3D-Var statistics files of the Danish Meteorological Institute (DMI). The climatological field, illustrated in Figure 2 (left), has a maximum over the Atlantic south of Greenland, where few observations were available in DMI's 3D-VAR analyses. This is also an area recognized for strong baroclinic developments (Petterssen, 1956, page 268). As expected, minima are found over the dense conventional observation networks in Europe and North America.

To be able to represent the time dependent variations in the increased forecast uncertainties associated with cyclone developments, spatial variations in upper air throughs, jets and thermal gradients must be utilized. One objective way of measuring these variations is to apply the so-called Eady index, based on the ideas of Eady (1949), representing the maximum normal mode error growth rate in baroclinic disturbances (Lindzen and Farrell, 1980; Hoskins and Valdes, 1990):

$$\sigma_{BI} = 0.31 f \left| \partial V / \partial z \right| N^{-1} \tag{4}$$

where f is the Coriolis parameter, N the boyancy frequency, and dV/dz the vertical wind shear. The coefficient 0.3125 has been derived by analytical scaling and explicit numerical calculations, simulating the atmosphere using a quasi geostrophic model.

The Eady index approach (Lindskog *et al.*, 2006) has formed the basis for the introduction of a time dependent variation on synoptic scales of the background error standard deviations in HIRLAM 3D-Var. It is achieved by the horizontally varying index field described in eq. (4), calculated from forecasts of previous assimilation cycles. In the HIRLAM case the vertical levels of 300 hPa and 1000 hPa were used for calculating the vertical gradient of eq. (4). The local error standard deviations are assumed proportional to the error growth. The ability of the Eady based index field to capture variations in he synoptic flow is illustrated in Figure 2 (right).

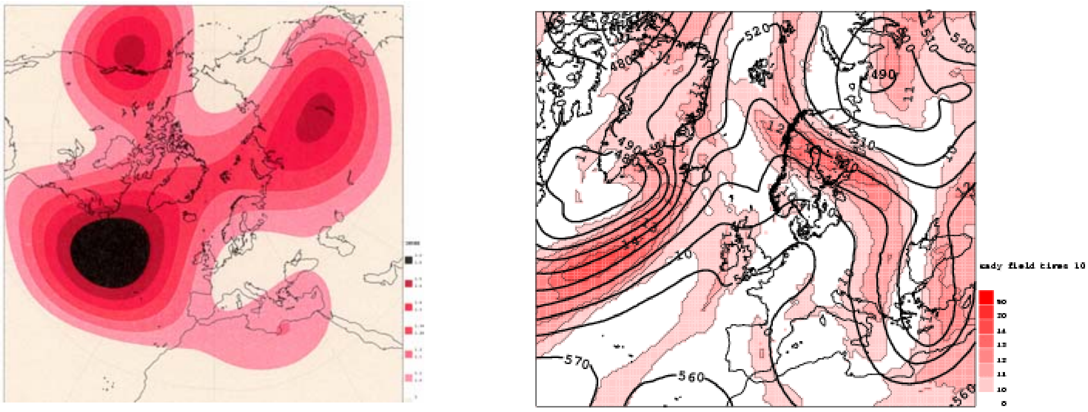

Figure 2: Climatological sigma-b index field (shaded red, left) and Eady based synoptically varying sigma-b index field (multiplied by ten, shaded red, right), together with 500 hPa geopotental height (gpm) of the background state (black isolines, right) valid at 20020105 18 UTC.

Parallel assimilation and forecasts experiments reveal a slightly positive impact of the improved representation of background error standard deviations on average verification statistics, as compared to neglecting the horizontal and temporal variation. There are however no significant difference between the forecasts utilising climatologically based and Eady based index fields, respectively. The time-averaged bias and rms scores for the one month of geopotential height and wind speed at the 700 and 200 hPa levels are shown in Figure 3.

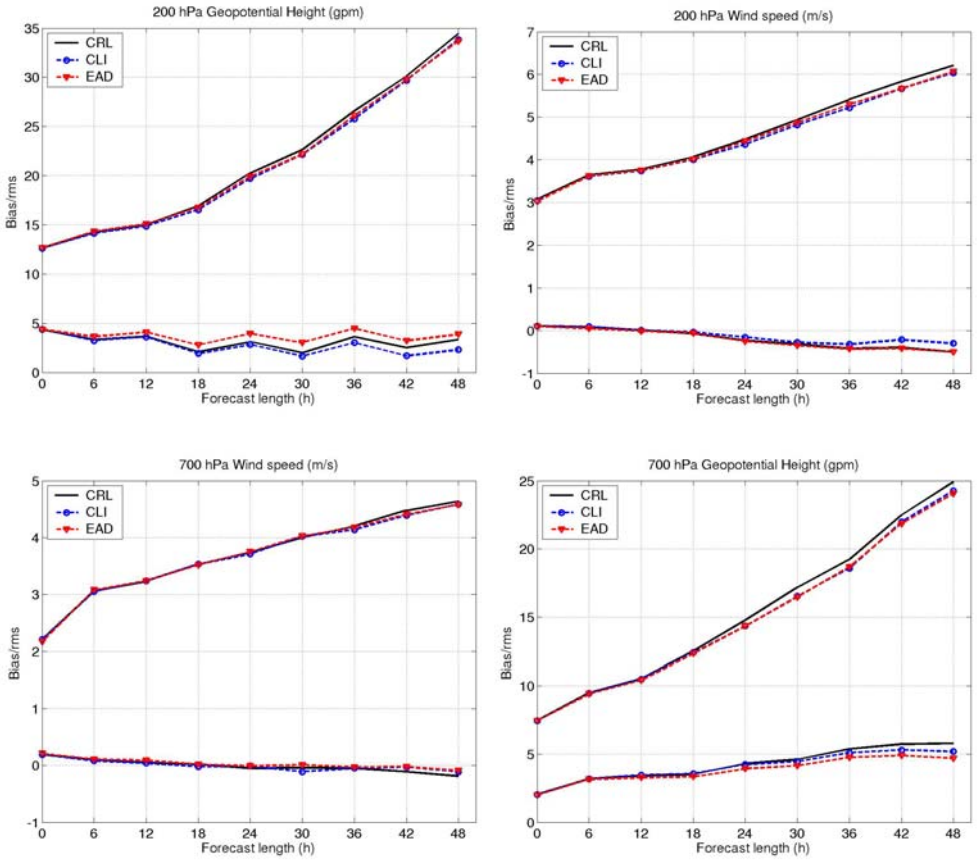

Figure 3: Rms and bias of geopotential height (gpm) and wind speed (m/s) forecasts as function of forecast length (h). Upper left: 200 hPa geopotential height. Lower left: 700 hPa geopotential height. Upper right: 300 hPa wnd speed. Lower right: 700 hPa wnd speed. Black lines are for run without horizontal sigma-b variation, blue for climatological sigma-b variation and red for Eady based sigma-b variation.

4. Flow dependent background error correlations

Two different methods are under development for obtaining a flow dependent representation of background error correlations. One is based on representing spatial variation and flow dependence by adapting a wavelet representation of an ensemble of short range forecasts and the other is based on obtaining flow dependency through including non-linear balance equations in the background constraint. It should also be mentioned that the new control variable for humidity, originally developed at ECMWF, is being included in the HIRLAM variational assimilation and results in a flow dependency. It should also be mentioned that 4D-Var itself implicitly results in a flow dependency.

4.1. Wavelet representation

In close collaboration with ALADIN the introduction of a complex wavelet transform constituting a tight frame (Kingsbury, 2001) is under development to represent the background error correlations.

This transform has two major advantages compared to the standard separable discrete wavelet transform (DWT). It is nearly shift invariant and nearly orientation invariant. This means that small translations or rotations of the signal will not result in great perturbations of the wavelet coefficients which simplifies further processing of the transform.

In the future statistics of real time forecast differences calculated from an ensemble of short range forecasts could be transformed into wavelet space, to obtain synoptically varying structure functions. To demonstrate this potential, statistics of 12 h minus 36 h forecasts valid at the same time were calculated for a number of 3-day periods (resulting in a sample of 12 cases of differences for each period), characterised by different synoptic flow situations. Figure 4 illustrates the 500 hPa geopotential height in the middle of two different periods. In Figure 5 the resulting wavelet representation of 500 hPa temperature derived background error correlations for the two cases is illustrated. Note how the correlations are elongated in the North-South direction, due to the front. For the second period the structure functions are less elongated but the length scales varies over the domain.

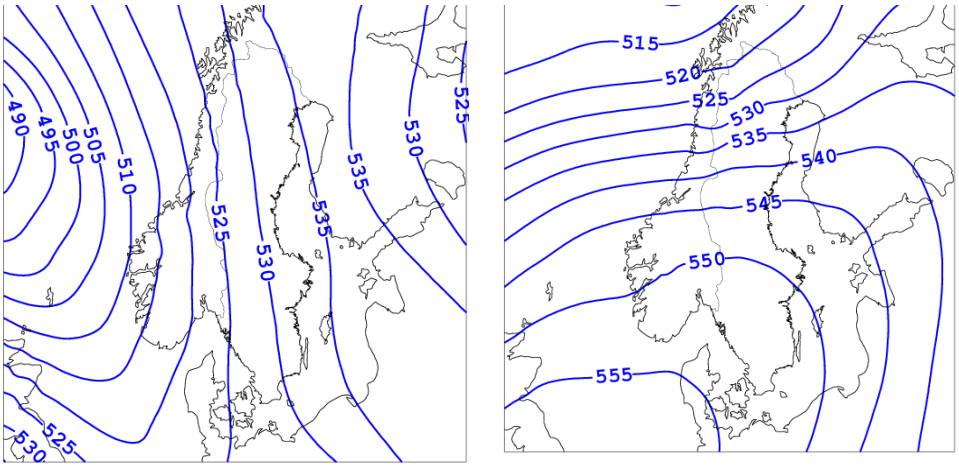

Figure 4: 500 geopotential height (gpm times 0.01) for 20060117 12 UTC (left) and 20060123 12 UTC (right).

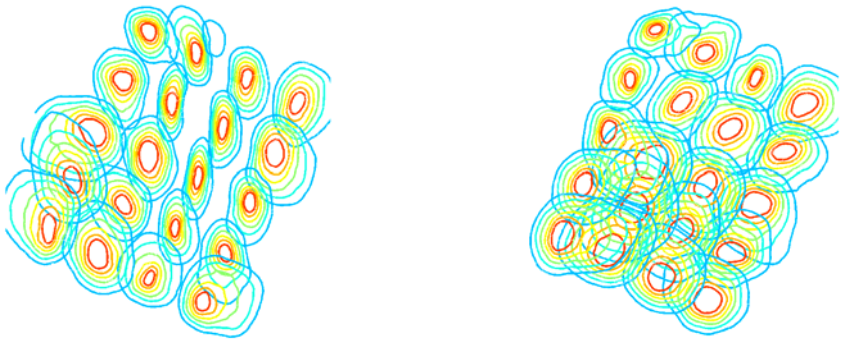

Figure 5: Wavelet representation of the horizontal correlations of 500 hPa temperature errors for the periods 20060116-20060118 and 20060122-20060124 (right).

4.2. Balance equations

The non-linear balance equation formulated on constant pressure levels may be formulated as

$$\nabla_p^2 \Phi = \left[f\nabla^2\psi + \frac{\partial f}{\partial x}\frac{\partial \psi}{\partial x} + \frac{\partial f}{\partial y}\frac{\partial \psi}{\partial y} + 2\frac{\partial^2\psi}{\partial x^2}\frac{\partial^2\psi}{\partial y^2} - 2\left(\frac{\partial^2\psi}{\partial x \partial y^2}\right)^2 \right]_p \qquad (5)$$

where f is the Coriolis parameter and ψ the streamfunction.

The tangent-linear version of equation (5) may be written as

$$\begin{aligned}\nabla_p^2\Phi' = f\left(\frac{\partial v_r'}{\partial x}-\frac{\partial u_r'}{\partial y}\right)_p + \frac{\partial f}{\partial x}v_r' + \frac{\partial f}{\partial y}u_r' \\ -2\left(\frac{\partial \overline{v}_r}{\partial x}\frac{\partial u_r'}{\partial y}+\frac{\partial \overline{u}_r}{\partial y}\frac{\partial v_r'}{\partial x}\right)_p + 2\left(\frac{\partial \overline{v}_r}{\partial y}\frac{\partial u_r'}{\partial x}+\frac{\partial \overline{u}_r}{\partial x}\frac{\partial v_r'}{\partial y}\right)_p\end{aligned} \tag{6}$$

with u_r, v_r being the rotational wind as calculated from the stream function. Primes represent assimilation increments and over-bars linearization points (first guess).

The tangent-linear version of the omega equation, formulated on constant pressure levels can be formulated

$$\sigma\nabla_p^2\omega' + f_0^2\frac{\partial^2\omega'}{\partial p^2} = -\nabla_p\cdot Q' + f_0\frac{\partial f}{\partial x}\frac{\partial u_g'}{\partial p} \tag{7}$$

with Q'_x and Q'_y defined as

$$Q_x' = -\frac{R_d}{p}\left[\frac{\partial \overline{u}_g}{\partial x}\frac{\partial T'}{\partial x}+\frac{\partial u_g'}{\partial x}\frac{\partial \overline{T}}{\partial x}+\frac{\partial \overline{v}_g}{\partial x}\frac{\partial T'}{\partial y}+\frac{\partial v_g'}{\partial x}\frac{\partial \overline{T}}{\partial y}\right]_p \tag{8}$$

$$Q_y' = -\frac{R_d}{p}\left[\frac{\partial \overline{u}_g}{\partial y}\frac{\partial T'}{\partial x}+\frac{\partial u_g'}{\partial x}\frac{\partial \overline{T}}{\partial x}+\frac{\partial \overline{v}_g}{\partial y}\frac{\partial T'}{\partial y}+\frac{\partial v_g'}{\partial x}\frac{\partial \overline{T}}{\partial y}\right]_p \tag{9}$$

where subscript g denotes geostrophic. Again, primes represent assimilation increments and over-bars linearization points (first guess).

Applications so far of the balance equation and the omega equation in the background error constraint have been based on the assumption that equations (5)-(9) are also approximately valid at model levels. Within HIRLAM considerable efforts have been spent on deriving the exact form of equations (5)-(9) on model levels and incorporating these in the background error constraint. When discretized, for HIRLAMs hybrid vertical coordinates, the system reduces to a linear system of equations of the form:

$$Ax = b \tag{10}$$

The incorporation in the background error constraint is not yet ready but to demonstrate the effect the balance equations have been introduced in the form of a weak constraint by adding an additional term, J_{be}, in the cost function:

$$J = J_b + J_o + J_{be} \tag{11}$$

where

$$J_{be} = \frac{1}{2}r^T W r = \frac{1}{2}\delta x L^T W L \delta x \tag{12}$$

where r is the residual, defined by:

$$\begin{bmatrix} r_\phi \\ r_\omega \end{bmatrix} = \begin{bmatrix} {}_{b_\phi} & A_\phi\delta\phi \\ b_\omega & A_\omega\delta\omega \end{bmatrix} = L\delta x \tag{13}$$

So far the weighting matrix, W, has been diagonal, but the residuals r_φ and r_ω have been scaled to have similar magnitude. The new term J_{be} preserves the quadratic form of the cost function since tangent-linear versions of the balance equations are used.

To illustrate the potential of introducing the J_{be} term, formulated on model levels a single temperature observation 5 K colder than the corresponding background equivalent and at the 925 hPa level and located in the Atlantic ocean west of Norway was introduced 20050107. The horizontal impact is illustrated in Figure 6, with and without the J_{be}. Note how this term, formulated on model levels prevents the observational information to spread over the mountains and into Norway. This feature is even more evident in Figure 7, which shows the corresponding cross-section in approximately the East-West direction. With the J_{be} term included the increments are more realistically spread. A similar single observation experiment has been carried out with all orographic terms in the J_{be} term set to zero, simulating applying the constant pressure level balance constraint (not shown). The resulting assimilation increments had a similar shape as when the J_{be} term was not added, confirming the importance of the orographic terms.

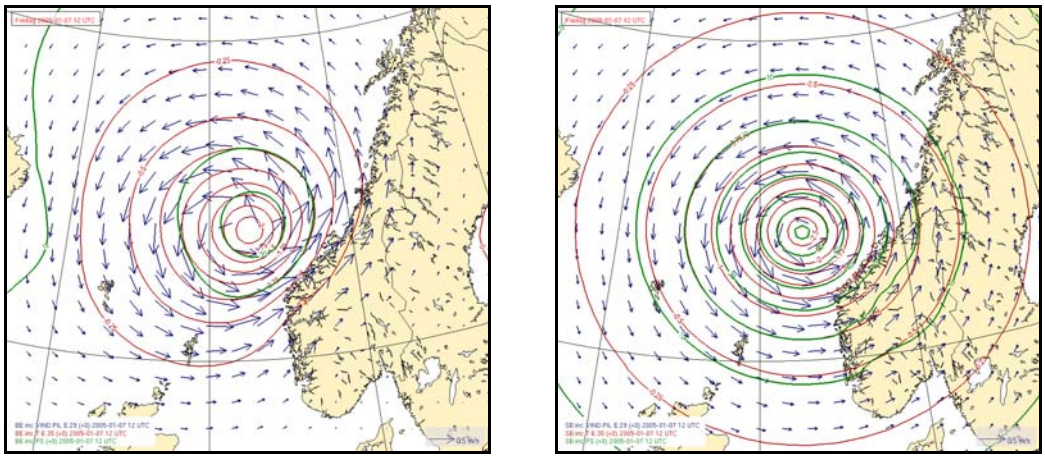

Figure 6: Assimilation increments due to one single temperature observation at 925 hPa, located over the Atlantic sea west of Norway and 5 K colder than the corresponding background state equivalent. Red isolines represents temperatures increments at 925 hPa, green isolines surface pressure increments and blue arrows wind increments. Left panel is when Jbe s not applied and right panel when it is applied.

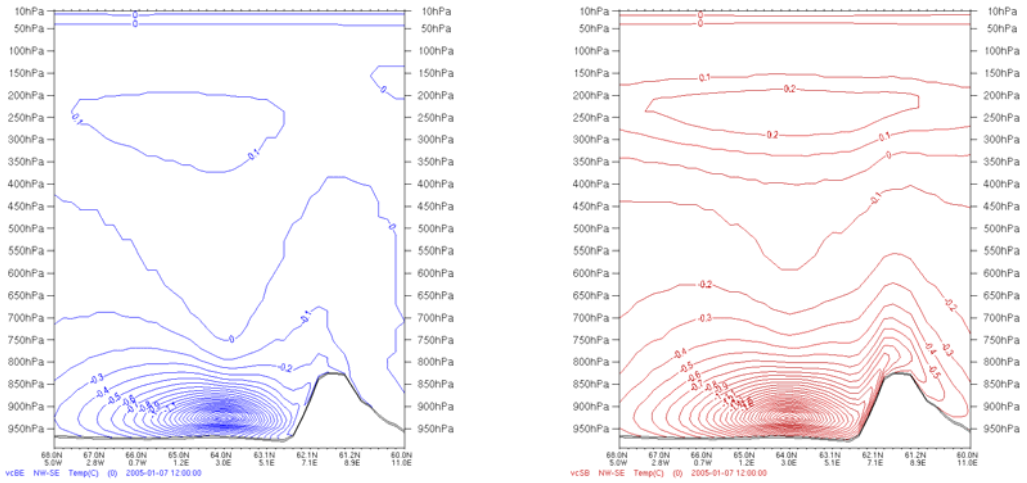

Figure 7: Temperature assimilation increments due to one single temperature observation at 925 hPa, located over the Atlantic sea west of Norway and 5 K colder than the corresponding background state equivalent. Vertical cross-section in East-West direction. Left panel is when Jbe is not applied and right panel when it is applied.

4.3. New humidity control variable

The present HIRLAM assimilation utilises specific humidity as control variable. Following developments at ECMWF we are in the process of replacing specific humidity with a new control variable, based on normalized relative humidity, δRH*, given by:

$$\delta RH^* = \delta RH / \sigma_b (RH_b + 0.5\ \delta RH) \qquad (14)$$

where RH_b, σ_b represents the relative humidity background and background error standard deviation, respectively and δRH represents the observation minus background difference.

The adaptation of the new control variable has been done for both the analytical and statistical background error balance formulations and evaluations are ongoing. The new control variable has the potential advantages that large areas of strong super-saturation are avoided and that a flow dependency of the background error humidity correlations is induced. These potential advantages of the new humidity control variable, as compared with the old one based on specific humidity, are illustrated in Figure 8, which illustrates the humidity field resulting from a full scale data assimilation, using an analytical balance.

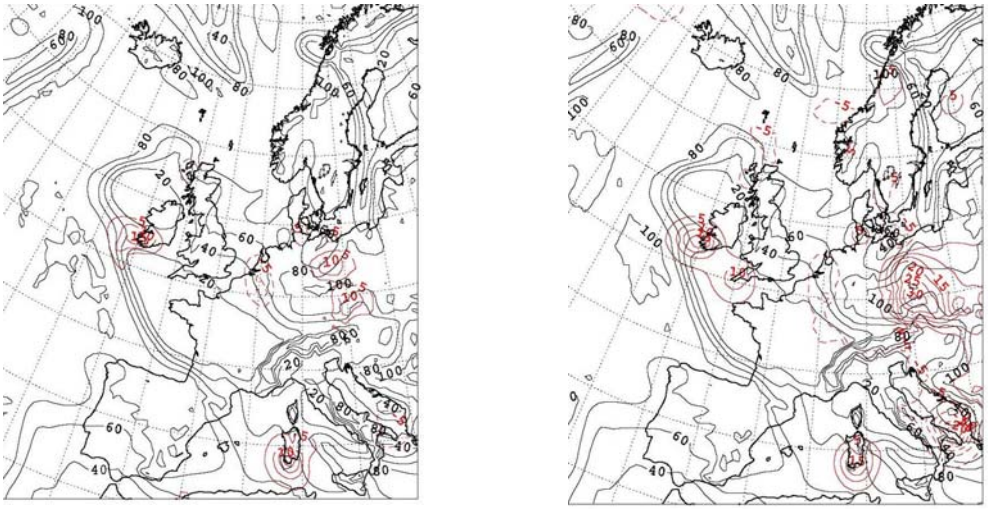

Figure 8: Relative humidity results with old (left) and new moisture control variable from full scale assimilation experiments, using an analytical balance, for 1 January, 2003, 06 UTC. Analysis and analysis increments at the 850 hPa level (black). Unit :%.

The statistical balance formulation of HIRLAM's variational data assimilation includes a multivariate formulation for humidity. Two avoid 'double counting' of the balance between humidity with surface pressure and temperature the control variable described by eq. (14) is slightly modified. Figure 9 shows the specific humidity and surface pressure assimilation increments due to 5 specific humidity observations, at the 850 hPa level, 10 g/kg lower than the corresponding background state equivalents. The differences in influence of the five observations on specific humidity (left panel) are due to differences in the background state. It can be seen (right panel) how the humidity observations also influence the surface pressure field, due to the multivariate humidity balance formulation. An observation error standard deviation of 1 g/kg was used for all simulated observations.

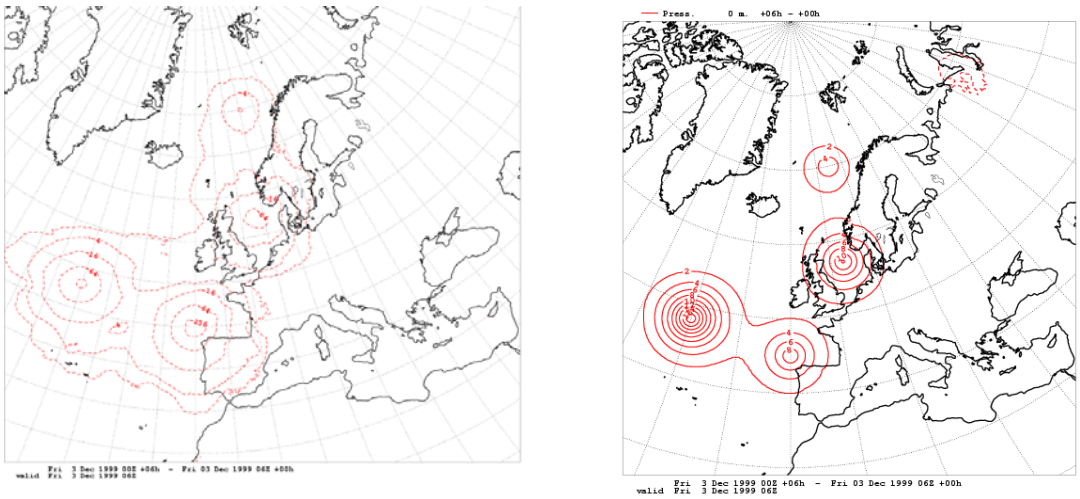

Figure 9: Assimilation increments due to five specific humidity simulated observations, at the 850 hPa level, 10 g/kg lower than the corresponding background state equivalents. Left panel shows the increments in specific humidity (g/kg times 10) and right panel on surface pressure (hPa times 10).

5. Summary

The background error constraint of HIRLAM's variational data assimiliation has been improved by introducing a statistical balance. A positive impact of introducing Eady-index based flow dependent background error standard deviations has been demonstrated. Research with encouraging preliminary results related to introduction of flow dependent background error correlations are ongoing. The two approaches investigated are a complex wavelet transform in combination with an ensemble assimilation system and introduction of non-linear balance equations in the background error constraint. Furthermore, a new moisture control variable originally developed at ECMWF, has been introduced into HIRLAM's variational data assimilation and results in flow dependent moisture background error correlations.

6. References

Berre, L. 2000. Estimation of synoptic and meso scale forecast error covariances in a limited area model. *Mon. Wea. Rev.*, **128**, 644-667.

Courtier, P., Thépaut, J.-N. and Hollingsworth, A. 1994. A strategy for operational implementation of *4D-Var using an incremental approach. Q. J. R. Meteorol. Soc.*, **120**, 1367-1388.

Gustafsson, N., Berre, L., Hörnquist, S., Huang, X.-Y., Lindskog, M., Navascués, B., Mogensen, K. S. and Thorsteinsson, S. 2001. Three-dimensional variational data assimilation for a limited area model. Part I: General formulation and the background error constraint. *Tellus*, **53A**, 425-446.

Hoskins B. J. and Valdes P. J. 1990. On the existence of storm tracks. *J. Atmos. Sci.,* **47**, 1854-1864.

Houtekamer, P.L., Lefaivre, L., Derome, J., Ritchie, H. And Mitchell, H. L. 1996. A System Simulation Approach to Ensemble Prediction. *Mon. Wea. Rev.*, **124**, 1225-1242.

Kingsbury N. G., 2002. Complex wavelets for shift invariant analysis and filtering of signals., *Journal of Applied and Computational Harmonic Analysis*, vol. **10**, no. **3**, 254-253.

Lindskog, M., Gustafsson, N., Navascués, B., Mogensen, K. S., Huang, X.-Y., Yang, X., Andræ, U., Berre, L., Thorsteinsson, S. and Rantakokko, J., 2001. Three-dimensional variational data assimilation for a limited area model. Part II: Observation handling and assimilation experiments. *Tellus*, **53A**, 447-468.

Lindskog M., Gustafsson, N. and Mogensen, K. S., 2006. Representation of background error standard deviations in a limited area model data assimilation system. *Tellus*, **58A**, 430-444.

Lindzen, R. S. and Farell, B. 1980. A simple Approximate Results for the Maximum Growth Rate of Baroclinic Instabilities. J. *Atmos. Sci.*, **37**, 1648-1654.

Parrish, D.F. and Derber, J.C., 1992: the National Meteorological Centre's spectral statistical interpolation analysis system. *Mon. Wea. Rev*., **120**, 1747-1763.

Petterssen, S. 1956. Weather Analysis and Forecasting, Second Edition, Volume I: Motion and Motion systems. McGraw-Hill Book Company Inc.